

Maximum Height and Return Point Velocities of Desalination Brine Discharges

A. T. Crowe, M. J. Davidson, R. I. Nokes

Department of Civil and Natural Resources Engineering
University of Canterbury, Christchurch 8140, New Zealand

Abstract

The effluent from reverse osmosis desalination plants consists mostly of hypersaline brine that is discharged back into the ocean. Inclined jets are commonly used to dispose of the negatively buoyant brine effluent at an upwardly inclined angle to horizontal. Commercial numerical model predictions underestimate dilution compared with experimental data. Therefore, the assumptions behind these models need to be examined. However, limited experimental velocity data exists. Particle tracking velocimetry laboratory experiments are conducted to obtain further velocity field information from negatively buoyant discharges. Non-dimensional centreline velocity is found to be linearly dependent on the initial densimetric Froude number. Maximum height and return point velocities are reported and compared to numerical model predictions for source angles of 30° , 45° , and 60° . Numerical models are found to overestimate centreline velocity for all angles.

Introduction

An increasing number of communities have water demand deficits as natural potable water sources become depleted and water consumption increases. A dependable potable water supply is important in semi-arid and arid regions where large periods of drought fail to replenish natural water sources. Desalination has become a viable method of supplementing the water supply through technological advances, reduced costs, and an increased desire to guarantee supply in many regions. Large desalination plants have been the preferred option in many countries including Saudi Arabia, UAE, Oman, Qatar, Israel, USA, Spain, and Australia [1].

Seawater reverse osmosis (SWRO) desalination involves desalting seawater to produce potable water. SWRO desalination plants are typically supplied with feedwater from the ocean through a pipeline, before pressure is applied to the feedwater on one side of a RO membrane filter, resulting in potable water and hypersaline brine on either side of the membrane. The brine is typically disposed of through an offshore ocean outfall using turbulent jets inclined upwards. Figure 1 illustrates the behaviour of a negatively buoyant brine jet discharged through a single source outlet. Initial momentum causes the discharge to rise through the water column to a maximum height before the negative buoyancy causes the discharge to fall downwards towards the seabed. The return point is the location where the discharge returns to the same elevation as the source outlet. Brine discharges can have significant impacts on the local marine environment and these impacts must be mitigated through appropriate design.

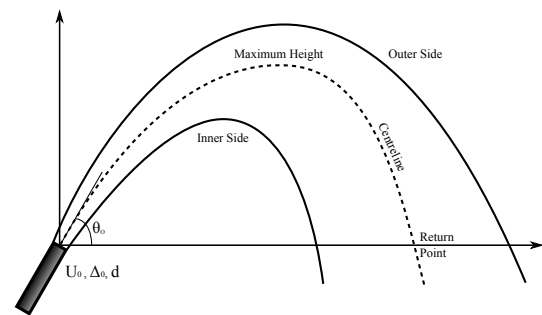


Figure 1: Trajectory of inclined negatively buoyant jet

Previous Research

The majority of experimental research has been conducted in laboratories with limited data available from field studies. Laboratory experiments, where the concentration field was measured, found the source angle of 60° produced the maximum discharge trajectory and dilution compared to 30° and 45° [9]. A 60° source angle then became the de facto standard for practical applications [8]. Inclined negatively buoyant jets have additional flow features that are not observed in positively buoyant discharges, such as municipal waste discharges. Here negatively buoyant describes discharges where the vertical component of the initial momentum flux is the opposite direction to the buoyancy force. Significant detrainment was observed on the inner side of inclined negatively buoyant jets due to the unstable stratification. This resulted in an asymmetry of the observed cross-sectional profiles [3]. A significant interaction occurs between rising and falling sides of these discharges for source angles above 75° , with the falling side deflected towards the rising side due to the strong entrainment near the source outlet [2].

Commercial numerical models, such as CORMIX (CORJET) and VISJET, employed in the design of inclined negatively buoyant discharges have been developed to model positively buoyant jets [6]. These models numerically integrate a system of simple ordinary differential equations that relate to the volume, momentum, and buoyancy fluxes of turbulent jets and plumes. The models have been extensively verified for positively buoyant jets. However, differences exist between model predictions and experimental results for negatively buoyant jets. Figure 2 shows the significant underestimation of dilution by these models at the return point when compared to experimental data. Detrainment enhances mixing with the ambient fluid on the inner side of the negatively buoyant discharges, which models do not consider.

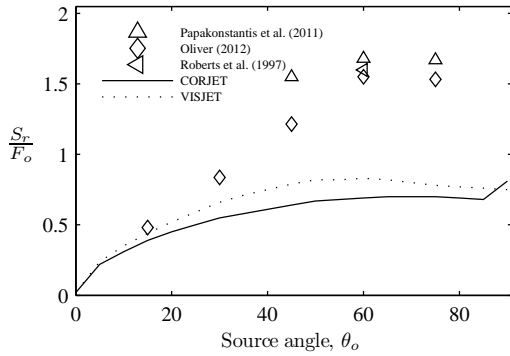


Figure 2: Return point dilution [7, 5, 8]

For a given discharge angle the flow behaviour is governed by the initial densimetric Froude number (equation 1).

$$F_o = \frac{U_o}{\sqrt{\Delta_o d}} \quad (1)$$

where U_o is the initial discharge velocity, Δ_o is the initial reduced buoyancy, and d is the internal diameter of the source outlet.

Numerous studies have measured concentration fields to determine the dilution of these discharges, however there have been limited velocity field experiments. The purpose of the present study is to provide further velocity field information from inclined negatively buoyant jets using particle tracking velocimetry (PTV) at the practically relevant source angles (θ_o) of 30° , 45° , and 60° . Eight experiments were conducted for each source angle, for a range of Froude numbers in a stationary ambient fluid.

Experimental Method

As noted above, PTV was the non-intrusive flow visualization technique employed for the scaled laboratory experiments. This technique involved seeding the discharged and ambient fluids with 125-180 μm pliolite resin tracer particles that have a similar density to water. The tracer particles were illuminated using a 2 W laser that was reflected onto a 16,000 RPM rotating mirror, which reflected light onto a parabolic mirror producing a thin sheet of light that passed directly through the centre of the discharge. The motion of particles was recorded by a JAI Pulnix TM-2030CL CCD greyscale video camera located perpendicular to the discharge as shown in figure 3. The JAI camera is a greyscale progressive scan scientific camera that allows manual control of shutter speed, gain, offset, and video depth to produce quality low light digital images. The location of tracer particles in each image was recorded by the video camera, allowing the velocity to be determined by the change in location of the particles between images. The velocity of the fluid can be directly inferred from the velocity of the small particles as they are fully mixed.

The experiments were conducted in a glass sided tank with dimensions; 2.30 m wide, by 1.78 m high, by 1.23 m deep. The discharged fluid had a density approximately 3 % greater than the ambient tap water. The discharged fluid was created by adding salt (NaCl) to tap water and was gravity fed to the source outlet from a constant head tank. The experimental tank was left to settle before each experiment such that ambient conditions were quiescent. The volumetric flow rate was digitally logged from an electromagnetic flow meter so that the source conditions could be determined accurately. The lower boundary of

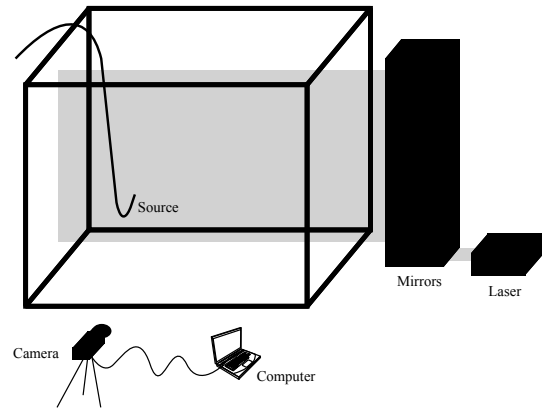


Figure 3: Configuration of experimental system

the experimental tank was sufficiently far from the source outlet such that it had no influence on the observed behaviour.

Raw images were captured from the video camera at 32 Hz through a CameraLink interface by a Correco capture card and written to a high speed hard drive. The raw images were converted to bitmap images before being analysed using Streams software [4]. Typically 9600 images (5 minutes) of each experiment were analysed. Each experiment was analysed in two sections of 4800 images each and concatenated together due to random access memory (RAM) limitations of the computers used. The location of tracer particles was determined in every image through a particle identification process. The locations of tracer particles are matched between consecutive images based on an auctioning algorithm using multiple conditions. Figure 4 shows the successful particle matches where the turbulent mixing behaviour of these discharges is evident. The velocity of matched tracer particles was determined and velocities were then interpolated onto a regular grid. A mean (time averaged) velocity field is shown in figure 5. A MATLAB algorithm was written to extract maximum height and return point velocities from the mean field.



Figure 4: Particle matches across 16 images (0.5 seconds)

Experimental Results

Cross-sectional velocity profiles were taken perpendicular to the maximum (centreline) velocity of the discharge at maximum height and the return point. Figure 6 shows the axial and normal velocities at maximum height that have been non-dimensionalised by the centreline velocity, u_c . The radial distance from the centreline, r , was non-dimensionalised by the discharge width, b . The discharge width is defined as the radial distance from the centreline velocity to where the velocity is equal to $e^{-1}u_c$. Negative r/b values refer to the outer side of

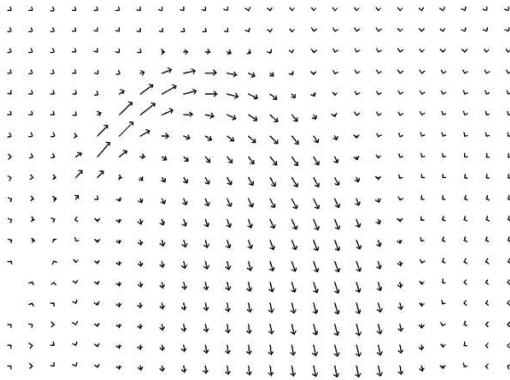


Figure 5: Mean velocity field, $\theta_o = 60^\circ$

the flow. The velocity profiles are asymmetrical about the centreline. Non-dimensional velocity profiles are similar at maximum height for the eight experiments conducted at 45° . Axial velocities on the outer side of the discharge have a Gaussian form. The axial velocity distribution is non-Gaussian on the inner side, where conditions are unstably stratified. Normal velocities on the inner side are negative and larger than the axial velocities indicating significant detrainment of discharged fluid is occurring at maximum height.

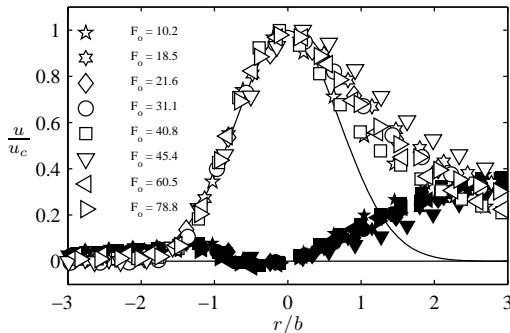


Figure 6: Velocity profiles at maximum height for $\theta_o = 45^\circ$, unfilled: axial, filled: normal

Non-dimensional axial and normal velocities at the return point are shown in figure 7. The non-dimensional velocity profiles are again asymmetrical and similar across all eight experiments. Axial velocities on the outer side retain a Gaussian form. Axial velocities on the inner side are large and decay in a near linear way from the centreline. The motion of detrained fluid is primarily downwards due to its negative buoyancy. This motion is in a similar direction to the centreline velocity at the return point, resulting in the large axial velocities on the inner side. The normal velocities on the inner side are still negative indicating that detrainment is still occurring at the return point. Non-dimensional velocity profiles at maximum height and return point showed the same characteristics for 30° and 60° .

Dimensional analysis determined that the centreline velocity should be non-dimensionalised by the initial discharge velocity. This non-dimensional parameter was found to be dependent on the Froude number and source angle. Figure 8 shows the non-dimensional centreline velocities at maximum height and the return point for a range of Froude numbers. Non-dimensional centreline velocity is found to be directly proportional to Froude number at both these locations. The same behaviour was observed for the source angles of 30° and 60° . Therefore, an empirical coefficient that is independent of source conditions can

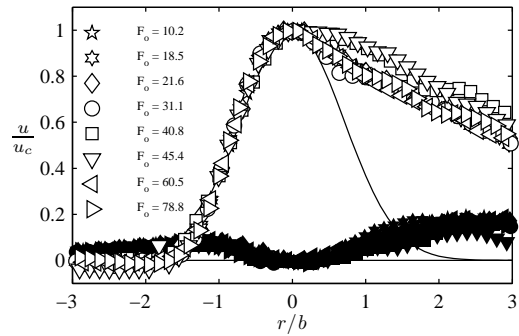


Figure 7: Velocity profiles at return point for $\theta_o = 45^\circ$, unfilled: axial, filled: normal

be determined by dividing the non-dimensional centreline velocity by the respective Froude number for each experiment.

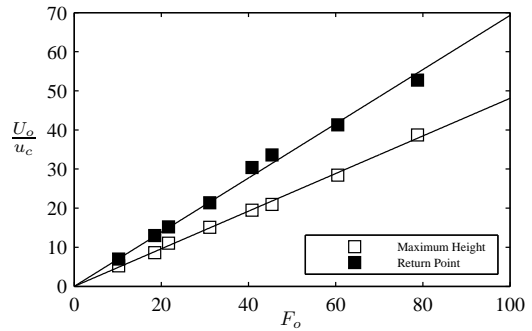


Figure 8: Centreline velocity at maximum height and the return point for $\theta_o = 45^\circ$

The empirical coefficient was averaged across all experiments for each source angle at the return point. Figure 9 compares the empirical coefficient determined from the experiments with the value predicted by commercial numerical models. The models are shown to significantly overestimate the centreline velocity at the return point for all angles studied. The experimental data shows that the empirical coefficient increases with source angle, whereas numerical models predict that this coefficient is relatively constant for source angles above 30° . These experimental results for velocity are consistent with behaviour shown in figure 2. As the discharge mixes into the ambient fluid, the dilution increases the centreline velocity decreases. Detrainment on the inner side of the discharge increases the mixing with the ambient, which the models do not consider, as previously noted.

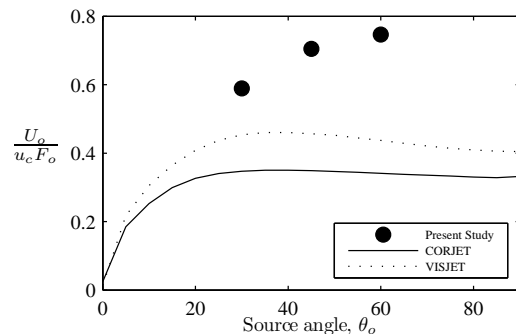


Figure 9: Comparison of return point centreline velocity

Conclusions

PTV experiments have been employed to obtain high quality velocity field information from inclined negatively buoyant jets. Non-dimensional velocity profiles were asymmetrical and similar across a range of different Froude numbers. Velocity profiles at maximum height and return point show detrainment occurring on the inner side of these discharges. Axial velocities on the outer side of the discharge have a Gaussian form at maximum height and the return point. Axial velocities on the inner side have a non-Gaussian form. Non-dimensional centreline velocity at maximum height and the return point were found to be directly proportional to Froude number. Numerical models overestimated centreline velocity at the return point for all angles studied, which is consistent with behaviour observed in previously measured concentration data.

References

- [1] Bleninger, T. and Jirka, G. H., Environmental planning, prediction and management of brine discharges from desalination plants, Technical Report 2nd Periodic Report, Middle East Desalination Research Center, 2009.
- [2] Ferrari, S. and Querzoli, G., Mixing and re-entrainment in a negatively buoyant jet, *Journal of Hydraulic Research*, **48**, 2010, 632–640.
- [3] Lane-Serff, G., Linden, P. and Hillel, M., Forced, angled plumes, *Journal of Hazardous Materials*, **33**, 1993, 75–99.
- [4] Nokes, R., *Streams Version 2.00 System Theory and Design*, 2012.
- [5] Oliver, C. J., *Near Field Mixing of Negatively Buoyant Jets*, Ph.D. thesis, University of Canterbury, 2012.
- [6] Palomar, P., Lara, J., Losada, I., Rodrigo, M. and Alvarez, A., Near field brine discharge modelling part 1: Analysis of commercial tools, *Desalination*, **290**, 2012, 14 – 27.
- [7] Papakonstantis, I. b., Christodoulou, G. and Papanicolaou, P., Inclined negatively buoyant jets 2: Concentration measurements, *Journal of Hydraulic Research*, **49**, 2011, 13–22.
- [8] Roberts, P. J. W., Ferrier, A. and Daviero, G., Mixing in inclined dense jets, *Journal of Hydraulic Engineering*, **123**, 1997, 693–699.
- [9] Zeitoun, M. A., Conceptual designs of outfall systems for desalting plants, Technical report, 1970.